



This is a repository copy of *Numerical modelling and design of normal and high strength steel non-slender welded I-section beam–columns*.

White Rose Research Online URL for this paper:

<https://eprints.whiterose.ac.uk/198058/>

Version: Published Version

Article:

Zhu, Y., Yun, X. orcid.org/0000-0002-5179-4731 and Gardner, L. (2023) Numerical modelling and design of normal and high strength steel non-slender welded I-section beam–columns. *Thin-Walled Structures*, 186. 110654. ISSN 0263-8231

<https://doi.org/10.1016/j.tws.2023.110654>

Reuse

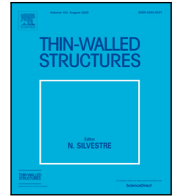
This article is distributed under the terms of the Creative Commons Attribution-NonCommercial-NoDerivs (CC BY-NC-ND) licence. This licence only allows you to download this work and share it with others as long as you credit the authors, but you can't change the article in any way or use it commercially. More information and the full terms of the licence here: <https://creativecommons.org/licenses/>

Takedown

If you consider content in White Rose Research Online to be in breach of UK law, please notify us by emailing eprints@whiterose.ac.uk including the URL of the record and the reason for the withdrawal request.



eprints@whiterose.ac.uk
<https://eprints.whiterose.ac.uk/>



Numerical modelling and design of normal and high strength steel non-slender welded I-section beam–columns

Yufei Zhu ^a, Xiang Yun ^{b,*}, Leroy Gardner ^a

^a Department of Civil and Environmental Engineering, Imperial College London, London SW7 2AZ, UK

^b Department of Civil and Structural Engineering, The University of Sheffield, Sheffield S1 3JD, UK

ARTICLE INFO

Keywords:

Beam–columns
Combined loading
Finite element (FE) modelling
High strength steel (HSS)
In-plane member stability
Normal strength steel (NSS)
Welded I-section

ABSTRACT

This paper presents a comprehensive numerical study into the in-plane member stability and design of normal and high strength steel (NSS and HSS) non-slender welded I-section beam–columns subjected to compression plus uniaxial bending. Finite element (FE) models were firstly developed to replicate the structural performance of welded I-section beam–columns made of different steel grades, as observed in existing tests collected from the literature. The validated FE models were then employed in a comprehensive parametric study to generate extensive numerical data covering a wide range of cross-section geometries, steel grades, member slendernesses and loading combinations. The numerically obtained data were utilised to evaluate the accuracy of the current design methods set out in the European Standards EN 1993-1-1:2005 and EN 1993-1-12:2007 as well as the American Specification AISC 360-16 for both NSS and HSS non-slender welded I-section beam–columns. The comparisons revealed that the codified design methods yield varying levels of accuracy in predicting the ultimate capacities of welded I-section beam–columns depending on the steel grade. To address this issue, new design proposals that are compatible with the European beam–column design framework have been developed, featuring more accurate yield strength-dependent interaction curves anchored to improved resistance predictions for members subjected to isolated loading scenarios (i.e. the compression and bending end points of the interaction curves). The new design proposals have been found to provide more accurate and consistent resistance predictions than the existing codified design provisions for NSS and HSS non-slender welded I-section members under compression plus uniaxial bending. The reliability of the new proposals has been confirmed through statistical analyses according to EN 1990: 2002.

1. Introduction

High strength steels (HSS), with yield strengths equal to or greater than 460 N/mm², are becoming increasingly popular in construction for heavily loaded structural members in high-rise buildings, bridges and stadia. The use of HSS can lead to significant weight savings, resulting in lower CO₂ emissions and energy use (i.e. directly because of the lower steel consumption and indirectly due to reduced transportation and handling costs). Despite the advantages of HSS, use in structures remains relatively low; this is partly due to shortcomings and limitations in the existing design rules. The current codified design provisions for HSS structures, as set out in the European Standard EN 1993-1-12:2007 (EC3) [1] and the American Specification AISC 360-16 [2], are generally a simple extension of the design rules for normal strength steels (NSS), without considering the full influence of the yield strength on the behaviour and design of steel structures made of varying steel grades. In addition, the majority of the existing design provisions are applicable to the design of steel structures made of steel grades up to S700, while steel grades above S700 are generally not

covered. It is thus imperative to develop more accurate, efficient and reliable design rules for HSS structures.

To date, a number of studies have been carried out to investigate the structural behaviour and design of NSS and HSS welded I-section stub columns [3–8], beams [9–12] and columns [13–18]. A trend of a reducing relative influence of imperfections (both the global geometric imperfections and residual stresses) on member buckling resistance with increasing steel grades has been revealed in these studies. However, the observed behaviour is only partially captured in the current EC3 design approach and in design proposals put forward in the literature by applying different imperfection factors for welded I-section columns made of different steel grades in a step-wise manner. Specifically, a lower imperfection factor corresponding to a higher buckling curve is used for HSS than for NSS columns. To address the discrete nature of the existing approaches, a modified imperfection factor expressed in terms of the material factor $\epsilon = \sqrt{235/f_y}$ was proposed by [16] for the design of welded I-section columns made of steel grades varying from S235 to S960, taking due account of

* Corresponding author.

E-mail address: x.yun@sheffield.ac.uk (X. Yun).

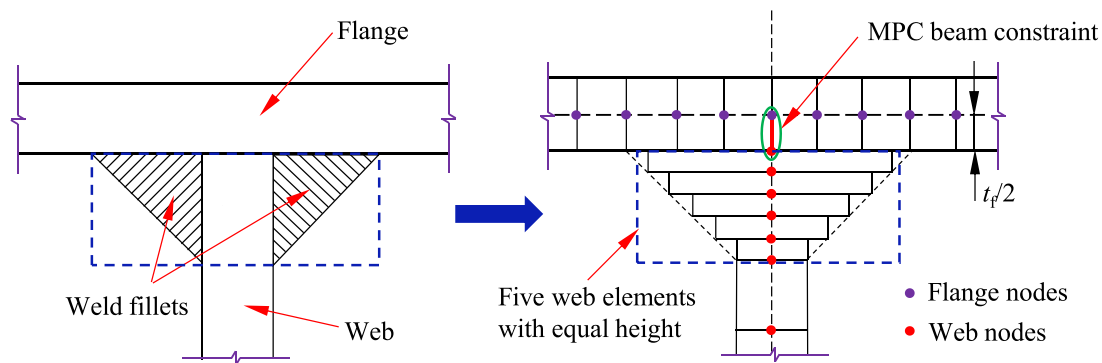


Fig. 1. Modelling technique for geometrical representation of weld fillets in welded I-sections.

the influence of yield strength on the column buckling behaviour in a consistent and continuous manner. Previous investigations into the structural response and design of NSS and HSS welded I-section beam-columns remain scarce. Su et al. [19] experimentally and numerically studied the local-global buckling interaction response of S960 steel beam-columns with slender welded I-sections and developed a new design method. Yang et al. [20] and Ma et al. [21,22] carried out a series of tests on non-slender welded I-section beam-columns made of Q460 steel and Q690 steel, respectively, subjected to compression plus minor axis bending. They concluded that the accuracy of the existing EC3 design rules for HSS non-slender welded I-section beam-columns could be improved by introducing higher flexural buckling curves. More recently, Tse et al. [23] performed a numerical study into the structural behaviour of S690 and S960 steel non-slender welded I-section beam-columns under compression plus uniaxial bending and proposed a modified EC3 design method for these members, providing more accurate and consistent resistance predictions than the current EC3 provisions. However, this proposed modified EC3 design approach was only validated for welded I-section beam-columns made of S690 and S960 steels.

This paper presents an extension of the previous study [16] with a focus on the in-plane stability design of non-slender (i.e. Class 1–3, according to the slenderness limits set out in prEN 1993-1-1:2019 [24]) welded I-section beam-columns considering the influence of steel grade. Finite element (FE) models that can replicate the structural response of NSS and HSS welded I-section beam-columns were developed and validated against experimental results collected from the literature [20,21]. Upon validation, the FE models were employed in extensive parametric studies to generate an FE data pool covering a broad range of cross-section geometries, steel grades, member slendernesses and loading combinations. The generated FE results, as well as the existing test results, were used to evaluate the accuracy of the codified design rules for NSS and HSS welded I-section beam-columns set out in the European Standards EN 1993-1-1 [24,25] and EN 1993-1-12 [1], and the American Specification AISC 360-16 [2]. Shortcomings in the existing design rules were revealed, which promoted the establishment of a new design approach for welded I-section beam-columns with varying steel grades up to S960. The design proposals are based on newly developed flexural buckling curves for determining the column buckling strengths [16] and the Continuous Strength Method (CSM) [26,27] for calculating the cross-sectional bending resistances, serving as the end points of the design interaction curves for beam-columns. The proposed method permits a systematic consideration of the influence of yield strength and harmonises the equations for the in-plane stability design of welded I-section beam-columns made of varying steel grades, and is shown to provide significantly improved accuracy and consistency in the resistance predictions of welded I-section beam-columns compared with the existing codified design provisions. Finally, the reliability of the proposed design approach is assessed by performing statistical analyses according to EN 1990:2002 [28].

2. Numerical modelling programme

A comprehensive numerical modelling programme was performed to generate extensive numerical data on welded I-section beam-columns made of NSS and HSS using the FE analysis package ABAQUS [29]. The basic modelling assumptions and validation of the FE models are described in Sections 2.1 and 2.2, respectively, while the parametric studies are reported in Section 2.3.

2.1. FE modelling assumptions

The four-noded doubly curved shell element S4R with reduced integration and finite membrane strains was used throughout the numerical simulations in this paper; this element has been successfully employed in previous numerical studies [12,16,22,23] regarding the modelling of welded I-section structural elements. The cross-sectional mesh size was taken as the minimum of $(B+H)/40$ and the flange thickness t_f , where B is the flange width and H is the outer section depth. The adopted cross-sectional mesh size was also assigned uniformly along the longitudinal direction of the modelled members so that the aspect ratio of the elements were close to unity. Weld fillets were explicitly modelled by using five web elements with equal height but varying thicknesses, as illustrated in Fig. 1. The thicknesses of these web elements were determined in the validation study such that the cross-sectional area of each FE model was equal to that of the corresponding test specimen. This modelling technique has also been employed in the previous studies on hot-rolled [30] and welded I-sections [16,31,32]. Note that, for simplicity, weld fillets are not considered in the parametric studies.

The symmetric nature of the beam-column specimens enabled only half of each member length to be modelled, with longitudinal symmetry boundary conditions applied at mid-length, to improve the computational efficiency, as shown in Fig. 2. For ease of application of boundary conditions, the nodes at the end section of the FE model were coupled to a reference point by means of kinematic coupling, where pinned in-plane and fixed out-of-plane boundary conditions were simulated in accordance with the experiments. The reference point was offset from the centre of the end section longitudinally by a distance of $e_{0,x}$ to represent the distance between the specimen end and the tip of the knife-edge, and laterally by a distance of $e_{0,y}$ (or $e_{0,z}$) to consider the applied loading eccentricity in the major axis (or minor axis) direction according to the experiments, as shown in Fig. 2. The engineering stress-strain curves, measured from the tensile coupon tests in [20,21], were converted into true stress-logarithmic plastic strain curves before inputting into ABAQUS.

Both global and local geometric imperfections were introduced into the FE models by adjusting initial nodal coordinates of the perfect geometry. The global geometric imperfections were defined in the form of a half-sine wave shape along the longitudinal direction of the beam-column specimens. Sinusoidal local geometric imperfections were incorporated into the FE models with a half-wavelength

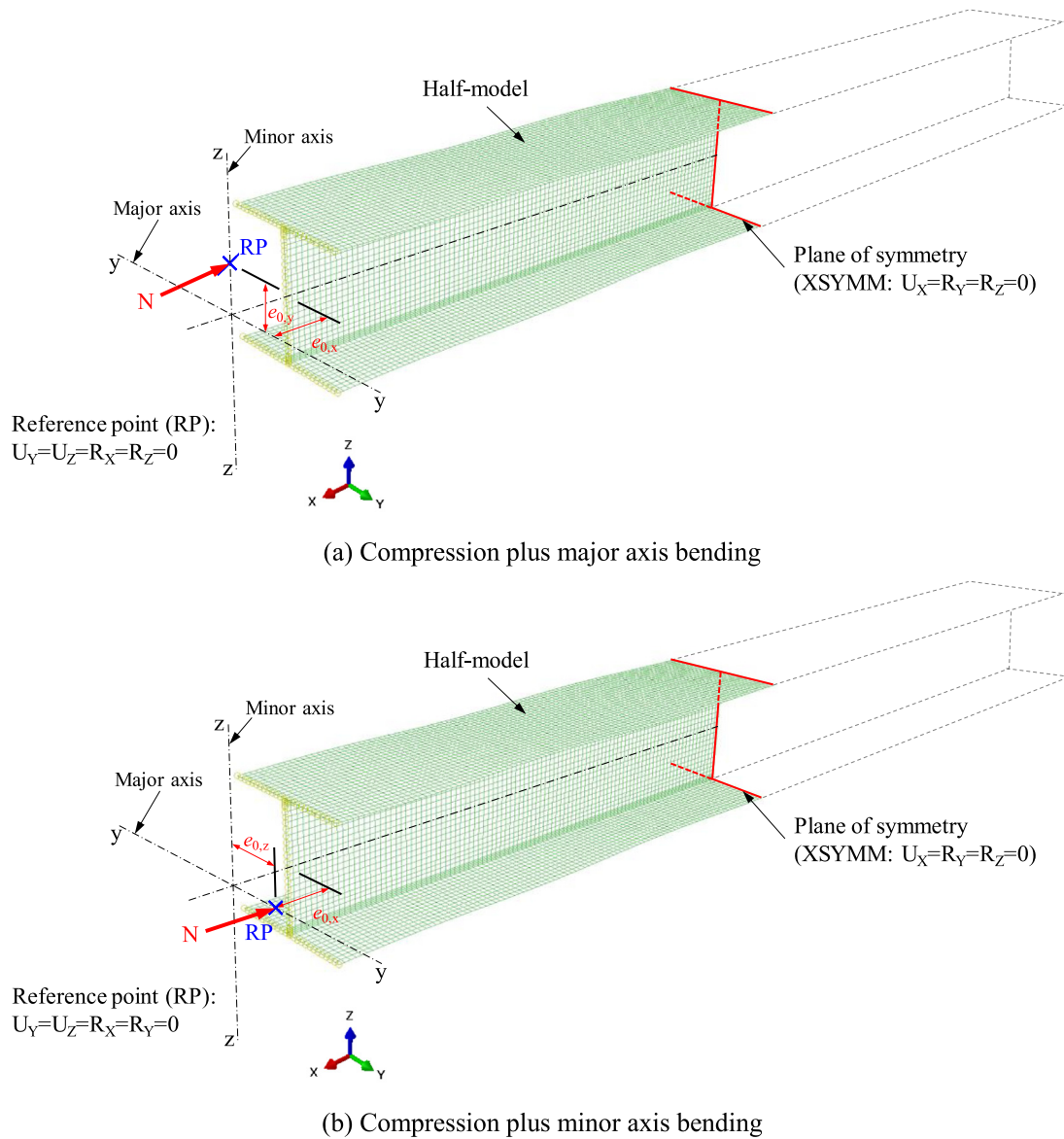


Fig. 2. Loading and boundary conditions of FE models of welded I-section beam-columns.

approximately equal to the elastic local buckling half-wavelength of the cross-section in compression $L_{b,cs}$, as shown in Fig. 3; the elastic local buckling half-wavelength was determined by using the simplified formulae developed by Fieber et al. [33]. Note that the determined elastic local buckling half-wavelength $L_{b,cs}$ was modified in order to fit an odd number of half-waves within the full member length, ensuring that the maximum local imperfection amplitudes were always located at the mid-length section where the symmetry boundary conditions were defined. The amplitudes of the local imperfections were taken equal to the fabrication tolerance-based values recommended in Annex C of EN 1993-1-5 [34], as indicated in Fig. 3, where δ_f and δ_w are the tolerance-based local imperfection amplitudes of the flanges and the web, respectively, t_w is the web thickness, b_f is the clear width of the outstand flange and h_w is the clear height of the web. More details about the adopted tolerance-based local geometric imperfections can be found in [12,16,35].

Residual stresses were introduced into the FE models using the residual stress pattern proposed in [16] by means of the ABAQUS *INITIAL CONDITIONS command. The proposed residual stress distribution for welded I-sections made of steel grades ranging from S235 to S960 is illustrated in Fig. 4, where $f_{r,fc}$ and $f_{r,wc}$ are the maximum compressive

residual stresses in the flanges and the web, respectively, and $f_{r,ft}$ and $f_{r,wt}$ are the maximum tensile residual stresses in the flanges and the web, respectively. The maximum tensile residual stresses $f_{r,ft}$ and $f_{r,wt}$ can be determined from Eq. (1) or Eq. (2):

$$\frac{f_{r,wt}(f_{r,ft})}{f_y} = -0.5 \times \sqrt{\frac{f_y}{235}} + 1.32 \leq 1 \quad (1)$$

$$\frac{f_{r,wt}(f_{r,ft})}{f_y} = -0.5 \times \sqrt{\frac{f_y}{235}} + 1.5 \leq 1 \quad (2)$$

which correspond approximately to the mean and upper characteristic (i.e. 95th percentile) values from an analysed experimental database [16], respectively. The maximum compressive residual stresses $f_{r,fc}$ and $f_{r,wc}$ can be accordingly determined considering force equilibrium within the cross-section. Eqs. (1) and (2) indicate a trend of decreasing relative residual stress amplitudes with increasing steel grades, the influence of which on the ultimate capacities of welded I-section beam-columns has not yet been fully explored. The proposed residual stress pattern is suitable for welded I-sections fabricated by means of gas metal arc welding (GMAW), which is one of the most common types of welding, and has been successfully employed in previous numerical simulations of NSS and HSS welded I-section beams [12] and

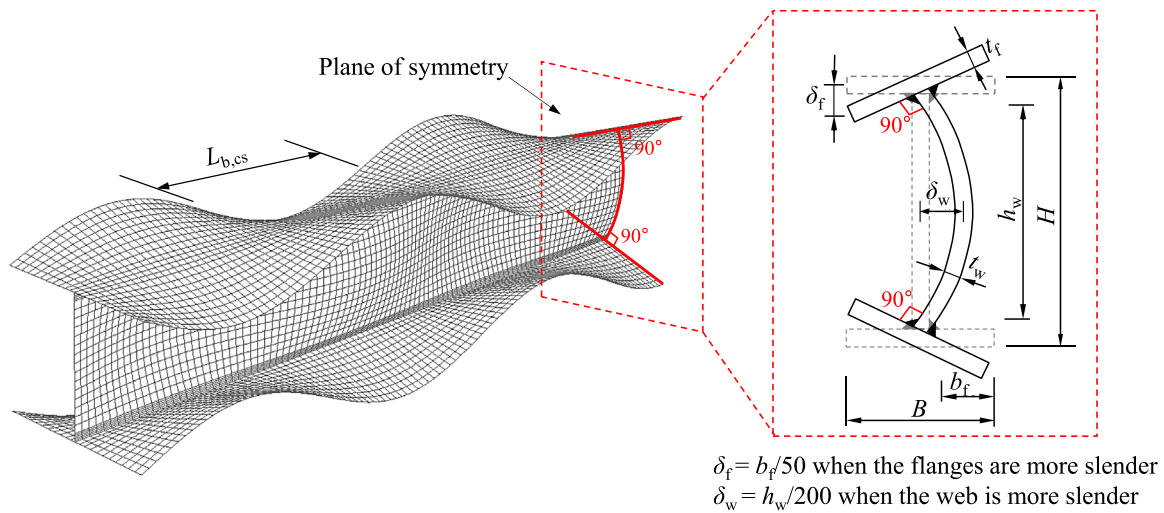


Fig. 3. Shape and amplitudes of local geometric imperfections employed in FE models.

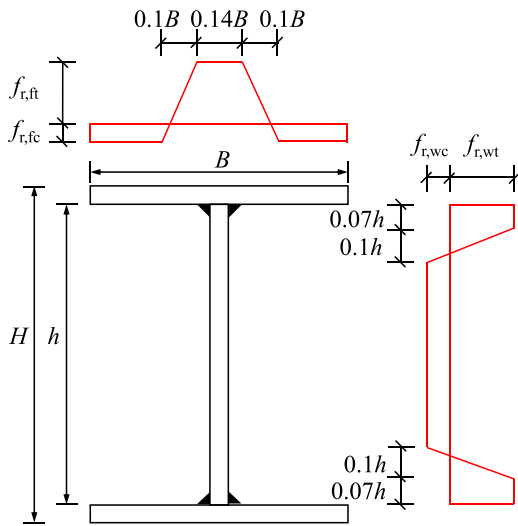


Fig. 4. Residual stress pattern [16] employed in FE models.

columns [16]. It was suggested [16] that the residual stress pattern with mean values of $f_{r,ft}$ and $f_{r,wt}$ obtained using Eq. (1) should be used for the validation of FE models, while the residual stress pattern with upper characteristic (95th percentile) values of $f_{r,ft}$ and $f_{r,wt}$ determined from Eq. (2) should be adopted for parametric studies. Considering both material and geometrical nonlinearities, the modified Riks method was employed in order to capture the full load–deformation histories of the beam–column specimens.

2.2. Validation of developed FE models

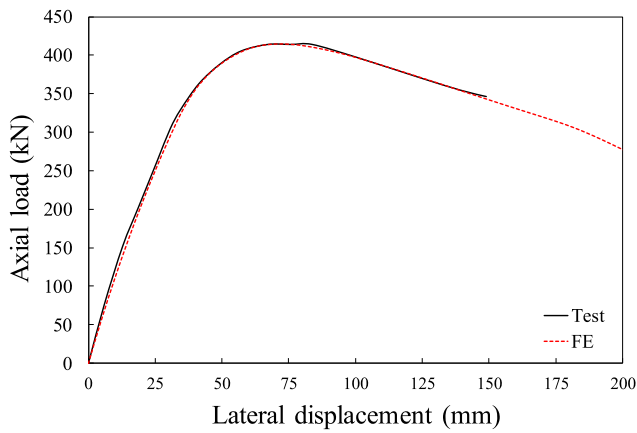
The developed FE models were validated by comparing the derived numerical predictions with the key experimental results obtained from a total of sixteen tests on welded I-section beam–columns under compression plus minor axis bending [20,21], including the axial load–lateral displacement histories, ultimate loads and failure modes. The comparisons between the ultimate loads derived from the FE simulations $N_{u,FE}$ and those obtained from the tests $N_{u,test}$ considering varying global imperfection amplitudes are summarised in Table 1, where the corresponding mean values and coefficients of variation (COV) of the ratios of $N_{u,FE}/N_{u,test}$ are also provided. The comparisons in Table 1

Table 1

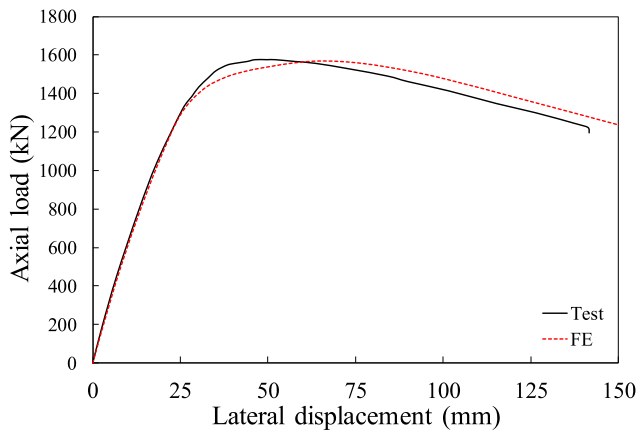
Comparisons of test and FE ultimate loads with varying levels of global imperfections.

Steel grade	Specimen label	$N_{u,FE}/N_{u,test}$			
		Global imperfection amplitude ω_g			Measured value
		$L_c/1000$	$L_c/1500$	$L_c/2000$	
Q460GJ [20]	H-314-30	0.962	0.969	0.973	0.981
	H-314-60	0.991	0.998	1.001	1.008
	H-266-45	0.983	0.991	0.995	1.005
	H-266-75	0.991	0.998	1.001	1.009
	H-218-30	0.909	0.919	0.924	0.934
	H-218-60	0.990	0.998	1.002	1.002
	H-170-45	1.014	1.023	1.027	1.031
	H-170-75	1.077	1.084	1.087	1.091
	Mean	0.990	0.997	1.001	1.008
COV	0.048	0.046	0.046	0.044	
S690 steel [21]	EH1P	0.941	0.945	0.946	0.950
	EH1Q	1.009	1.014	1.016	1.020
	EH2P	0.940	0.943	0.945	0.949
	EH2Q	0.991	0.996	0.998	1.002
	EH3P	0.977	0.980	0.982	0.988
	EH3Q	0.961	0.965	0.967	0.969
	EH4P	0.962	0.966	0.968	0.970
	EH4Q	0.954	0.959	0.961	0.967
	Mean	0.967	0.971	0.973	0.977
COV	0.025	0.025	0.025	0.025	

reveal that the load carrying capacities of welded I-section beam–columns are generally insensitive to the variation in global imperfection amplitudes (ω_g), and the test ultimate loads $N_{u,test}$ can be generally well predicted by the developed FE models for all four investigated global imperfection amplitudes. The FE models with the global imperfection amplitude ω_g taken as $L_c/1000$ (where L_c is the distance between the knife edges at the member ends), which is the level of global imperfection assumed in the development of the column buckling design rules in EC3 [1,24,25], were found to predict accurate, yet slightly conservative load carrying capacities since both the global and local imperfection amplitudes adopted in the FE models (i.e. the fabrication tolerance-based values [34] shown in Fig. 3) are generally higher than those measured in the experiments. Comparisons of the experimentally and numerically obtained axial load–lateral displacement curves for typical tested beam–columns are shown in Fig. 5, demonstrating that the full structural response of the members can be well replicated by the FE models. Failure modes obtained from the FE models were also found to be in good agreement with the physical failure modes observed in the corresponding tested beam–column specimens, as shown in Fig. 6.



(a) Q690 steel welded I-section beam-column (Specimen EH2Q [21])



(b) Q460GJ steel welded I-section beam-column (Specimen H-218-60 [20])

Fig. 5. Comparisons of typical test and FE load–deformation histories (with a global imperfection amplitude of $L_c/1000$) for welded I-section beam–columns under compression plus bending about the minor axis.

In general, the developed FE models may be seen to be able to provide accurate simulations of the structural behaviour of welded I-section beam–columns under compression plus minor axis bending and are thus deemed suitable for use in the following parametric studies.

2.3. Numerical parametric studies

Upon validation of the FE models, parametric studies were conducted to generate extensive structural performance data on NSS and HSS non-slender welded I-section beam–columns with varying steel grades, cross-section slenderness, member slenderness and loading combinations. A total of five steel grades were considered in the parametric studies—S235, S355, S460, S690 and S960. The bilinear plus nonlinear hardening material model developed by Yun and Gardner [36] was employed to generate the full-range stress–strain curves for the S235, S355, S460 and S690 steels, while the average measured stress–strain curve obtained from longitudinal tensile coupon tests in [37] was used for the S960 steel throughout the parametric studies. The measured stress–strain curve of the S960 steel [37] was employed since the scope of the bilinear plus nonlinear hardening material model developed in [36] is limited to steel grades up to S690. The basic material properties of the five investigated steel grades, including the Young's modulus E , the yield strength f_y , the ultimate tensile strength f_u and the ultimate strain ϵ_u corresponding to f_u are given in Table 2, and the full-range stress–strain curves of the five steel grades are displayed in Fig. 7. Note that the full-range stress–strain

Table 2

Basic material properties for five different steel grades adopted in parametric studies.

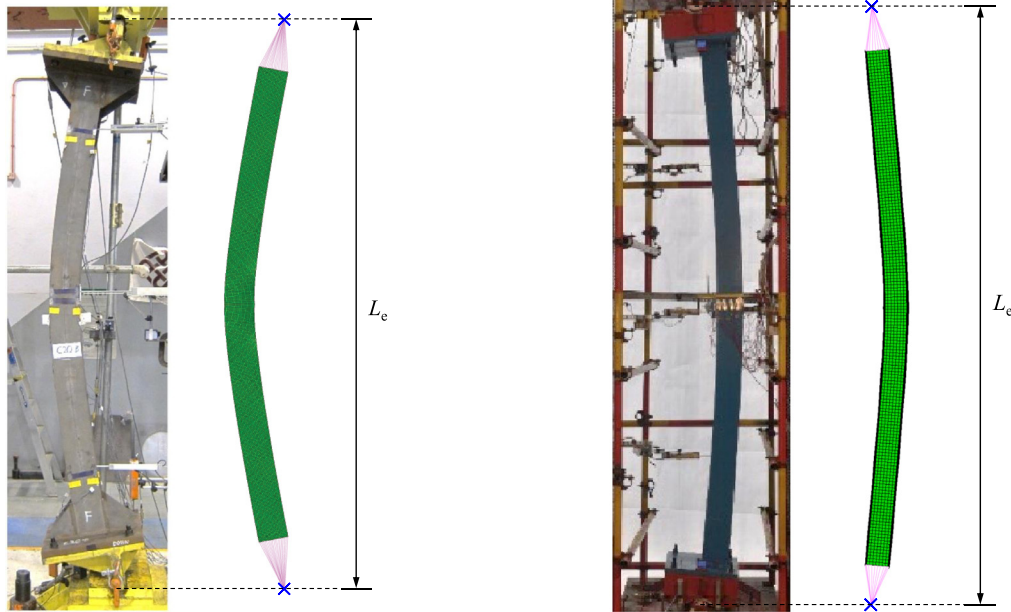
Steel grade	E N/mm ²	f_y N/mm ²	f_u N/mm ²
S235	210 000	235	360
S355	210 000	355	490
S460	210 000	460	540
S690	210 000	690	770
S960	204 393	969	1024

curves shown in Fig. 7 are all engineering stress–strains curves, which were transformed into true stress–logarithmic plastic strain curves prior to inputting into ABAQUS.

In the parametric studies, the flange width B was set equal to 100 mm, while three different outer section depths H were considered (i.e. 100 mm, 150 mm and 200 mm), leading to three cross-section aspect ratios H/B of 1.0, 1.5 and 2.0. For each cross-section aspect ratio, three different values of flange thickness t_f and web thickness t_w were selected to generate three different welded I-sections that covered all three non-slender cross-section classes (i.e. Class 1–3) according to the slenderness limits set out in prEN 1993-1-1 [24] and EN 1993-1-12 [1]. For each modelled cross-section, the thicknesses of the flanges t_f and the web t_w were chosen such that the flange plate slenderness $\lambda_{p,f}$ and the web plate slenderness $\lambda_{p,w}$ in compression, determined in accordance with EN 1993-1-5 [34], were approximately equal, thus minimising the effects of element interaction between the flange and the web [38]. Note that the weld fillets at each web–flange junction of the modelled I-sections were ignored in the parametric studies for modelling convenience. For each considered cross-section and for each axis of buckling, beam–column FE models with nine different lengths were selected to generate a wide spectrum of non-dimensional flexural buckling slenderness values $\bar{\lambda}$ from 0.2 to 2.6. For each beam–column FE model, a total of nine different initial loading eccentricities e_0 ranging between 1.1 mm and 4754 mm were considered to achieve a wide range of loading combinations (i.e. axial loading-to-bending moment ratios). For the beam–column FE models under compression plus major axis bending, out-of-plane lateral displacements were restrained at the web–flange intersections at regular intervals in order to suppress the flexural–torsional buckling effects. Throughout the parametric studies, the initial global and local geometric imperfection amplitudes were taken equal to $L_c/1000$ and the fabrication tolerance-based values (see Fig. 3) [34], respectively, while the residual stress pattern followed that shown in Fig. 4, with the upper characteristic maximum tensile residual stresses (determined from Eq. (2)). In total, 8290 FE data on NSS and HSS non-slender welded I-section beam–columns were generated, with half of the beam–columns subjected to compression plus major axis bending and the other half subjected to compression plus minor axis bending.

3. Assessment of existing design provisions for NSS and HSS welded I-section beam–columns

In this section, the current design provisions for NSS and HSS non-slender welded I-section beam–columns provided in the European design standards prEN 1993-1-1 [24] and EN 1993-1-12 [1], as well as the American Specification AISC 360-16 [2], are presented. The accuracy of each design method is assessed by comparing the numerically and experimentally obtained ultimate loads $N_{u,FE(test)}$ with those predicted by the design method $N_{u,pred}$, as reported in Table 3 and Table 4 for beam–columns under compression plus major and minor axis bending, respectively. A ratio of $N_{u,FE(test)}/N_{u,pred}$ greater than unity indicates that the design method provides a safe-sided resistance prediction and vice versa. Note that, in the assessment, all partial safety factors have been set equal to 1.0, thus facilitating a direct comparison between the FE (or test) ultimate loads $N_{u,FE(test)}$



(a) Q690 steel welded I-section beam-column (Specimen EH2Q [21]) (b) Q460GJ steel welded I-section beam-column (Specimen H-218-60 [20])

Fig. 6. Comparisons of typical test and FE failure modes for welded I-section beam-columns under compression plus bending about the minor axis.

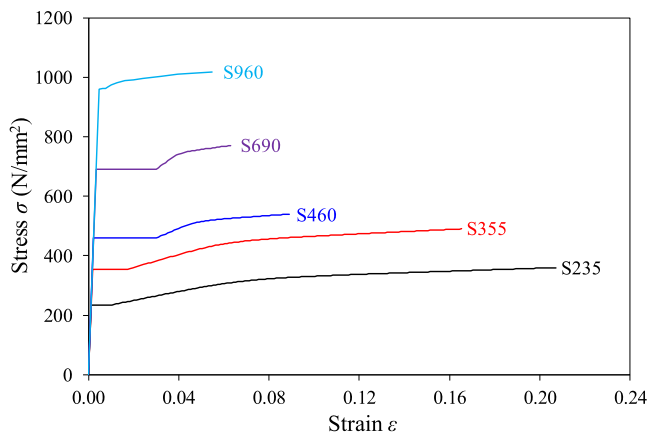


Fig. 7. Full-range stress-strain curves for five different steel grades adopted in parametric studies.

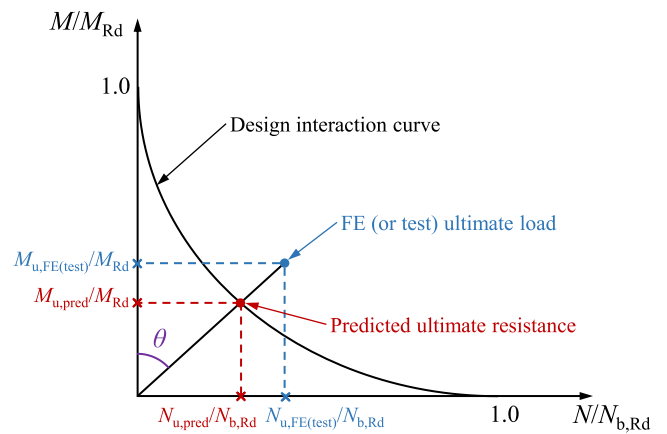


Fig. 8. Definition of the angle parameter θ on moment-axial compression ($M-N$) interaction curve.

and the strength predictions $N_{u,pred}$ obtained using the different design approaches. A dimensionless angle parameter θ is also introduced in the assessment to describe the relationship between the axial compressive load and the bending moment, as defined in Eq. (3) and illustrated in Fig. 8, in which $M_{u,FE(test)}$ is the numerical or experimental first order bending moment corresponding to the ultimate load $N_{u,FE(test)}$ (i.e. $M_{u,FE(test)} = N_{u,FE(test)}e_0$), and $N_{b,Rd}$ and M_{Rd} are the design resistances for column buckling and in-plane bending, respectively, determined in accordance with the considered design method. Note that $N_{b,Rd}$ and M_{Rd} represent the end points of the design interaction curve (i.e. the bending moment-axial load interaction curve), as shown in Fig. 8. The angle parameter θ varies between 0° to 90° , with $\theta = 0^\circ$ and $\theta = 90^\circ$ representing specimens subjected to bending alone and axial compression alone, respectively.

$$\theta = \tan^{-1} \left(\frac{N_{u,FE(test)}/N_{b,Rd}}{M_{u,FE(test)}/M_{Rd}} \right) = \tan^{-1} \left(\frac{M_{Rd}}{e_0 N_{b,Rd}} \right) \quad (3)$$

3.1. European standards prEN 1993-1-1 [24] and EN 1993-1-12 [1] (EC3)

According to the European design standards prEN 1993-1-1 [24] and EN 1993-1-12 [1], Eqs. (4) and (5) are given for the in-plane stability design of beam-columns with Class 1–3 welded I-sections under compression plus major axis bending and minor axis bending, respectively,

$$\frac{N_{Ed}}{N_{b,y,EC3}} + k_{yy,EC3} \frac{M_{y,Ed}}{M_{y,EC3}} \leq 1.0 \quad (4)$$

$$\frac{N_{Ed}}{N_{b,z,EC3}} + k_{zz,EC3} \frac{M_{z,Ed}}{M_{z,EC3}} \leq 1.0 \quad (5)$$

where N_{Ed} is the design axial compressive load, $M_{y,Ed}$ and $M_{z,Ed}$ are the design first order bending moments about the major and minor axes, respectively, $N_{b,y,EC3}$ and $N_{b,z,EC3}$ are the EC3 column flexural buckling resistances about the major and minor axes, respectively,

Table 3

Comparison of numerically obtained ultimate loads with those predicted using different design methods for welded I-section beam–columns under compression plus major axis bending.

Steel grade (No. of FE data)	Evaluation parameter	EC3 [24]	AISC [2]	New proposals
		$N_{u,FE}/N_{u,pred,EC3}$	$N_{u,FE}/N_{u,pred,AISC}$	$N_{u,FE}/N_{u,pred,prop}$
S235 (No. of FE: 729)	Mean	0.961	0.954	1.076
	COV	0.051	0.101	0.033
	Maximum	1.140	1.424	1.203
	Minimum	0.869	0.839	0.959
S355 (No. of FE: 729)	Mean	0.987	0.990	1.077
	COV	0.041	0.097	0.032
	Maximum	1.148	1.444	1.193
	Minimum	0.909	0.806	0.975
S460 (No. of FE: 729)	Mean	1.005	1.014	1.081
	COV	0.036	0.096	0.031
	Maximum	1.151	1.476	1.208
	Minimum	0.916	0.869	0.976
S690 (No. of FE: 729)	Mean	1.039	1.056	1.090
	COV	0.036	0.100	0.036
	Maximum	1.235	1.532	1.283
	Minimum	0.945	0.896	0.993
S960 (No. of FE: 729)	Mean	1.069	1.104	1.103
	COV	0.030	0.108	0.035
	Maximum	1.231	1.615	1.294
	Minimum	0.959	0.920	1.005
Overall (No. of FE: 3645)	Mean	1.012	1.024	1.085
	COV	0.054	0.113	0.035
	Maximum	1.235	1.615	1.294
	Minimum	0.869	0.806	0.959

Table 4

Comparison of numerically and experimentally obtained ultimate loads with those predicted using different design methods for welded I-section beam–columns under compression plus minor axis bending.

Steel grade (No. of FE/test data)	Evaluation parameter	EC3 [24]	AISC [2]	New proposals
		$N_{u,FE(test)}/N_{u,pred,EC3}$	$N_{u,FE(test)}/N_{u,pred,AISC}$	$N_{u,FE(test)}/N_{u,pred,prop}$
S235 (No. of FE: 729)	Mean	1.007	0.884	1.119
	COV	0.055	0.118	0.045
	Maximum	1.236	1.255	1.252
	Minimum	0.890	0.736	0.971
S355 (No. of FE: 729)	Mean	1.031	0.912	1.108
	COV	0.057	0.119	0.047
	Maximum	1.282	1.304	1.230
	Minimum	0.916	0.773	0.957
S460 (No. of FE: 729 No. of tests: 14)	Mean	1.051	0.932	1.113
	COV	0.056	0.117	0.047
	Maximum	1.283	1.308	1.267
	Minimum	0.923	0.779	0.977
S690 (No. of FE: 729 No. of tests: 4)	Mean	1.078	0.965	1.113
	COV	0.055	0.115	0.049
	Maximum	1.288	1.308	1.322
	Minimum	0.936	0.787	0.984
S960 (No. of FE: 729)	Mean	1.114	1.004	1.120
	COV	0.056	0.113	0.050
	Maximum	1.332	1.346	1.223
	Minimum	0.952	0.805	0.973
Overall (No. of FE: 3645 No. of tests: 18)	Mean	1.056	0.940	1.115
	COV	0.066	0.125	0.048
	Maximum	1.332	1.346	1.322
	Minimum	0.890	0.736	0.957

$M_{y,EC3}$ and $M_{z,EC3}$ are the EC3 cross-sectional bending resistances about the major and minor axes, respectively, and $k_{yy,EC3}$ and $k_{zz,EC3}$ are the EC3 interaction factors for beam–columns subjected to compression plus major and minor axis bending, respectively. Specifically, the EC3 flexural buckling resistance $N_{b,EC3}$ for columns with Class 1–3 welded I-sections can be determined from:

$$N_{b,EC3} = \chi_{EC3} A f_y, \tag{6}$$

where A is the gross cross-section area and χ_{EC3} is the EC3 flexural buckling reduction factor about the relevant buckling axis, as given by

Eqs. (7) and (8):

$$\chi_{EC3} = \frac{1}{\phi_{EC3} + \sqrt{\phi_{EC3}^2 - \bar{\lambda}^2}} \quad \text{but } \chi_{EC3} \leq 1.0 \tag{7}$$

$$\phi_{EC3} = 0.5 \left[1 + \alpha_{EC3} (\bar{\lambda} - 0.2) + \bar{\lambda}^2 \right] \tag{8}$$

in which $\bar{\lambda}$ is the column non-dimensional slenderness given by $\sqrt{A f_y / N_{cr}}$, where N_{cr} is the elastic buckling load about the relevant buckling axis, α_{EC3} is the EC3 imperfection factor, taken equal to 0.34 and 0.49 for both NSS and HSS welded I-section columns buckling

about the major and minor axes, respectively (i.e. corresponding to the EC3 column buckling curves “b” and “c”, respectively), though a recent study [39] recommended the use of revised column buckling curves “a” and “b” for the design of HSS columns buckling about the major and minor axes, respectively (i.e. imperfection factors α_{EC3} equal to 0.21 and 0.34, respectively).

With regards to the EC3 cross-sectional bending resistances M_{EC3} , prEN 1993-1-1 [24] prescribes the use of the plastic moment capacity M_{pl} (i.e. the product of the plastic section modulus W_{pl} and the yield strength f_y) for Class 1 and 2 welded I-sections, and the elasto-plastic moment capacity M_{ep} (i.e. the product of the elasto-plastic section modulus W_{ep} , as given by Eq. (9), and the yield strength f_y) for Class 3 welded I-sections. In accordance with the Annex B of prEN 1993-1-1 [24], W_{ep} is defined based on linear interpolation between W_{pl} and the elastic section modulus W_{el} with respect to the parameter β_{ep} , as given by Eq. (10):

$$W_{ep} = W_{pl} - (W_{pl} - W_{el}) \beta_{ep}, \quad (9)$$

$$\beta_{ep} = \begin{cases} \max\left(\frac{b_i/t_f - 10\epsilon}{4\epsilon}; \frac{h_w/t_w - 83\epsilon}{38\epsilon}; 0\right) \\ \leq 1.0, \text{ for bending about the major axis} \\ \max\left(\frac{b_i/t_f - 10\epsilon}{6\epsilon}; 0\right) \leq 1.0, \text{ for bending about the minor axis,} \end{cases} \quad (10)$$

where ϵ is the material parameter equal to $\sqrt{235/f_y}$. The EC3 interaction factors $k_{yy,EC3}$ and $k_{zz,EC3}$ for Class 1 to 3 welded I-sections can be determined from Eqs. (11) and (12), respectively. In Eqs. (11) and (12), C_{my} and C_{mz} are the equivalent uniform moment factors about the major and minor axes, respectively, which are equal to 1.0 for the investigated loading cases of uniform bending throughout the present study.

$$k_{yy,EC3} = \begin{cases} C_{my} \left[1 + (\bar{\lambda}_y - 0.2) \frac{N_{Ed}}{N_{b,y,EC3}} \right], \text{ for } \bar{\lambda}_y < 1.0 \\ C_{my} \left(1 + 0.8 \frac{N_{Ed}}{N_{b,y,EC3}} \right), \text{ for } \bar{\lambda}_y \geq 1.0 \end{cases} \quad (11)$$

$$k_{zz,EC3} = \begin{cases} C_{mz} \left[1 + (2\bar{\lambda}_z - 0.6) \frac{N_{Ed}}{N_{b,z,EC3}} \right], \text{ for } \bar{\lambda}_z < 1.0 \\ C_{mz} \left(1 + 1.4 \frac{N_{Ed}}{N_{b,z,EC3}} \right), \text{ for } \bar{\lambda}_z \geq 1.0 \end{cases} \quad (12)$$

The ratios of the ultimate loads obtained from the FE simulations and tests $N_{u,FE(test)}$ to the EC3 ultimate resistance predictions $N_{u,pred,EC3}$ are plotted against the corresponding angle parameter θ in Fig. 9(a) and (b) to investigate the accuracy of the EC3 design method for welded I-section beam-columns under compression plus major and minor axis bending, respectively. The overall mean and COV values of the load ratios $N_{u,FE(test)}/N_{u,pred,EC3}$ are equal to 1.012 and 0.054 for beam-columns under compression plus major axis bending, and equal to 1.056 and 0.066 for compression plus minor axis bending, as listed in Tables 3 and 4. It can be concluded from these statistical results and Fig. 9(a) and (b) that the current EC3 design method generally yields reasonable, but somewhat scattered ultimate resistance predictions for NSS and HSS non-slender welded I-section beam-columns, especially for those under compression plus minor axis bending. However, there are a set of data points of beam-columns under compression plus major axis bending lying on the unsafe side. The statistical results in Tables 3 and 4 also suggest that there is generally an increasing level of conservatism with increasing steel grade; this is due primarily to the neglect of the reducing relative influence of residual stresses on the ultimate resistance of beam-columns with increasing steel grades [16,23,40].

3.2. American specification AISC 360-16 [2] (AISC)

Eqs. (13) and (14) are given in the American Specification AISC 360-16 [2] (AISC) for the design of non-slender welded I-section beam-columns subjected to compression plus major and minor axis bending,

respectively, where $N_{b,y,AISC}$ and $N_{b,z,AISC}$ are the AISC column flexural buckling resistances about the major and minor axes, respectively, $M_{y,AISC}$ and $M_{z,AISC}$ are the AISC cross-sectional bending resistances about the major and minor axes, respectively, and α_{amp} is an amplification factor that accounts for the second-order effects in beam-column members, as given by Eq. (15).

$$\begin{cases} \frac{N_{Ed}}{N_{b,y,AISC}} + \frac{8}{9} \frac{\alpha_{amp} M_{y,Ed}}{M_{y,AISC}} \leq 1.0, \text{ if } \frac{N_{Ed}}{N_{b,y,AISC}} \geq 0.2, \\ \frac{N_{Ed}}{2N_{b,y,AISC}} + \frac{\alpha_{amp} M_{y,Ed}}{M_{y,AISC}} \leq 1.0, \text{ if } \frac{N_{Ed}}{N_{b,y,AISC}} < 0.2, \end{cases} \quad (13)$$

$$\begin{cases} \frac{N_{Ed}}{N_{b,z,AISC}} + \frac{8}{9} \frac{\alpha_{amp} M_{z,Ed}}{M_{z,AISC}} \leq 1.0, \text{ if } \frac{N_{Ed}}{N_{b,z,AISC}} \geq 0.2, \\ \frac{N_{Ed}}{2N_{b,z,AISC}} + \frac{\alpha_{amp} M_{z,Ed}}{M_{z,AISC}} \leq 1.0, \text{ if } \frac{N_{Ed}}{N_{b,z,AISC}} < 0.2, \end{cases} \quad (14)$$

$$\alpha_{amp} = \frac{1}{1 - (N_{Ed}/N_{cr})} \quad (15)$$

The AISC flexural buckling resistance $N_{b,AISC}$ for columns with non-slender welded I-sections can be expressed by Eq. (16), where χ_{AISC} is the AISC flexural buckling reduction factor about the relevant buckling axis, as given by Eq. (17).

$$N_{b,AISC} = \chi_{AISC} A f_y \quad (16)$$

$$\chi_{AISC} = \begin{cases} 0.658 \bar{\lambda}^{-2} \text{ for } \bar{\lambda} \leq 1.5 \\ \frac{0.877}{\bar{\lambda}^2} \text{ for } \bar{\lambda} > 1.5 \end{cases} \quad (17)$$

The AISC cross-sectional bending resistance M_{AISC} for compact cross-sections is the same as that for Class 1 and 2 cross-sections in EC3 [24] i.e. the plastic moment resistance M_{pl} , while an inelastic reserve method is used for noncompact cross-sections, which accounts for the effect of the partial spread of plasticity, as detailed in Section F of AISC 360-16 [2].

To assess the accuracy of the AISC beam-column design provisions, the FE and test ultimate loads $N_{u,FE(test)}$ are normalised by the AISC predicted ultimate resistances $N_{u,pred,AISC}$ and plotted against the corresponding angle parameter θ in Fig. 10(a) and (b) for the members under compression plus major and minor axis bending, respectively. The overall mean and COV values of the load ratios $N_{u,FE(test)}/N_{u,pred,AISC}$ are equal to 1.024 and 0.113 for beam-columns under compression plus major axis bending, and equal to 0.94 and 0.125 for compression plus minor axis bending, as provided in Tables 3 and 4. As can be seen from Fig. 10 and Tables 3 and 4, the AISC design method offers very scattered ultimate resistance predictions for both NSS and HSS non-slender welded I-section beam-columns, with a large number of data points falling on the unsafe side; this is attributed largely to the interaction curves adopted in AISC 360-16 [2].

4. New design proposals

The assessment presented in the previous section reveals that the current EC3 and AISC design methods provide somewhat inaccurate and scattered ultimate resistance predictions for NSS and HSS non-slender welded I-section beam-columns under compression plus uniaxial bending. Hence, new design proposals are set out in this section with the aim to achieve improved accuracy in the design of NSS and HSS non-slender welded I-section beam-columns. The new design proposals adopt the general format of the design interaction formulae specified in EN 1993-1-1 [24,25], with improvements made by employing more accurate end points (i.e. column flexural buckling strengths and cross-sectional bending resistances) and updated interaction factors.

4.1. New design formulae

The proposed design formulae are given in Eqs. (18) and (19) for NSS and HSS non-slender welded I-section beam-columns under

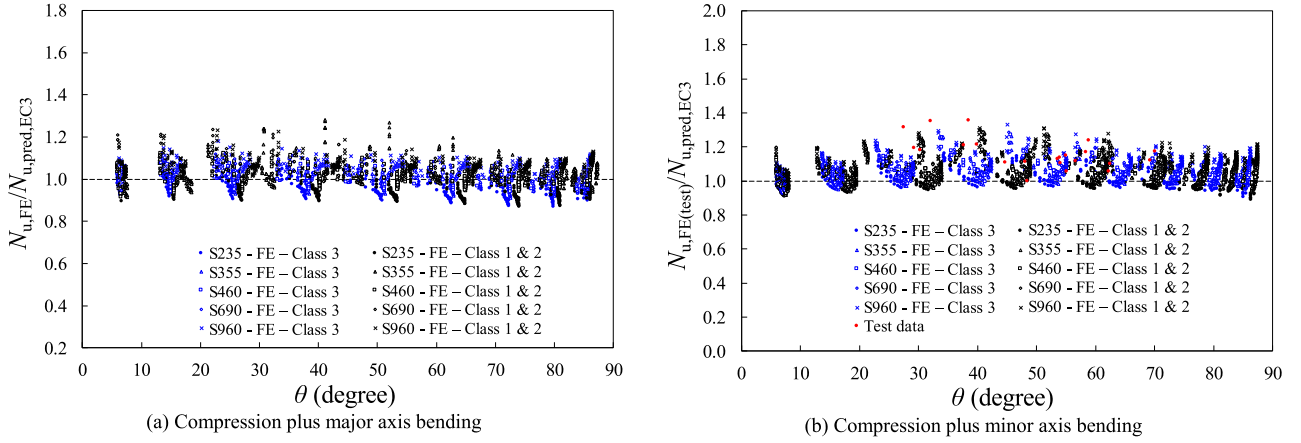


Fig. 9. Comparison of FE and test results with EC3 resistance predictions for NSS and HSS non-slender welded I-section beam-columns under combined loading.

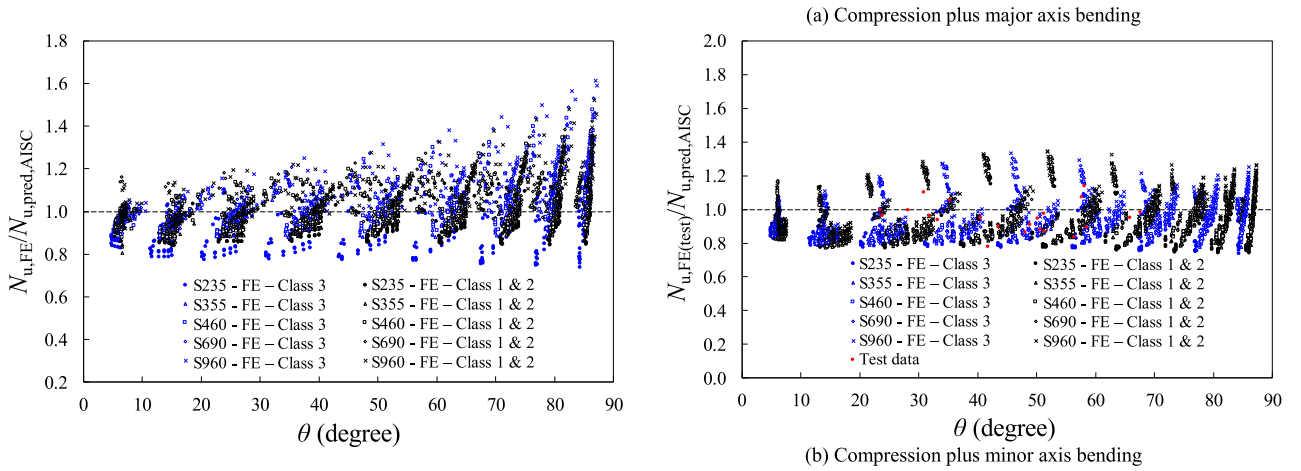


Fig. 10. Comparison of FE and test results with AISC resistance predictions for NSS and HSS non-slender welded I-section beam-columns under combined loading.

compression plus major and minor axis bending, respectively.

$$\frac{N_{Ed}}{N_{b,y,mod-EC3}/\gamma_{M1}} + k_{yy,prop} \frac{M_{y,Ed}}{M_{y,csm}/\gamma_{M1}} \leq 1.0 \quad (18)$$

$$\frac{N_{Ed}}{N_{b,z,mod-EC3}/\gamma_{M1}} + k_{zz,prop} \frac{M_{z,Ed}}{M_{z,csm}/\gamma_{M1}} \leq 1.0 \quad (19)$$

In Eqs. (18) and (19), $N_{b,y,mod-EC3}$ and $N_{b,z,mod-EC3}$ are the column flexural buckling resistances about the major and minor axes, respectively, determined using the modified EC3 column flexural buckling curves proposed by Yun et al. [16]. The modified EC3 flexural buckling resistances $N_{b,mod-EC3}$ for columns with Class 1–3 welded I-sections can be calculated using:

$$N_{b,mod-EC3} = \chi_{mod-EC3} A f_y, \quad (20)$$

where $\chi_{mod-EC3}$ is the modified EC3 flexural buckling reduction factor about the relevant buckling axis, as given by Eqs. (21) and (22):

$$\chi_{mod-EC3} = \frac{1}{\phi_{mod-EC3} + \sqrt{\phi_{mod-EC3}^2 - \bar{\lambda}^2}} \leq 1.0, \quad (21)$$

$$\phi_{mod-EC3} = 0.5 \left[1 + \alpha_{mod-EC3} (\bar{\lambda} - 0.1) + \bar{\lambda}^2 \right]. \quad (22)$$

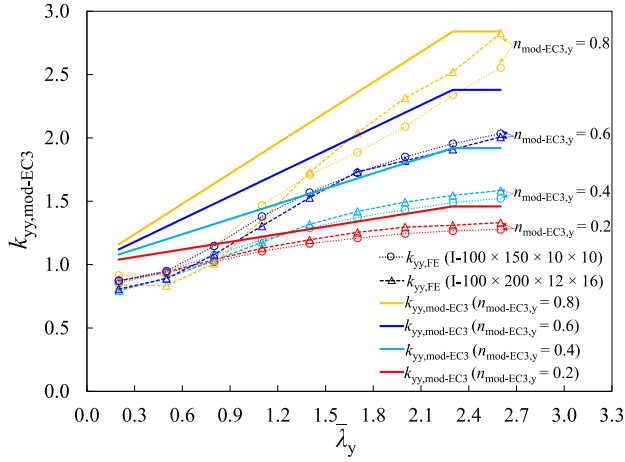
in which $\alpha_{mod-EC3}$ is the modified EC3 imperfection factor as given by Eqs. (23) and (24) for column flexural buckling about the major axis and minor axis, respectively, where ϵ is the material parameter equal to $\sqrt{235/f_y}$.

$$\alpha_{mod-EC3} = 0.45\epsilon, \text{ for flexural buckling about the major axis} \quad (23)$$

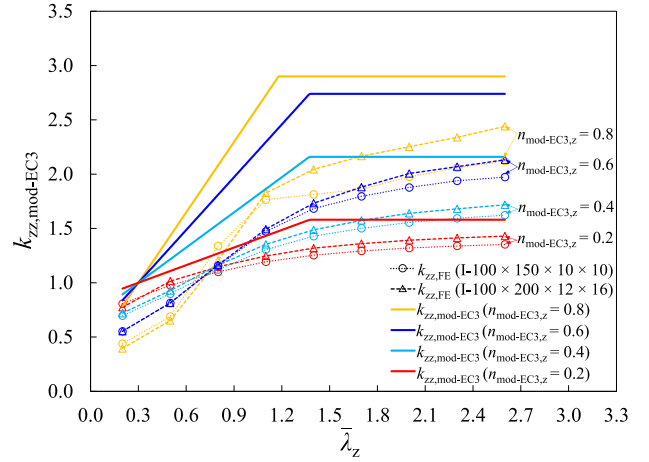
$$\alpha_{mod-EC3} = 0.55\epsilon, \text{ for flexural buckling about the minor axis} \quad (24)$$

The modified EC3 method has been shown to provide more accurate and consistent predictions of flexural buckling resistances for both NSS and HSS non-slender welded I-section columns than the current EC3 and AISC provisions [16], since the influence of yield strength on the flexural buckling resistances of welded I-section columns is rationally considered by using the modified imperfection factor $\alpha_{mod-EC3}$. The modified EC3 method [16] is therefore used to determine the compression end point (i.e. the column flexural buckling resistance) of the new design proposals for welded I-section beam-columns.

The bending end point of the new beam-column design proposals (i.e. the cross-sectional bending resistance about the major axis $M_{y,csm}$ in Eq. (18) or the minor axis $M_{z,csm}$ in Eq. (19)) is calculated by means of the Continuous Strength Method (CSM) [41–43], which enables a rational allowance to be made for material nonlinearity (i.e. the spread of plasticity and strain hardening) in the determination of cross-sectional resistances [26,27]. The CSM cross-sectional resistances for I-sections in major axis bending $M_{y,csm}$ and minor axis bending $M_{z,csm}$ are given by Eqs. (25) and (26), respectively, where ϵ_y is the material yield strain equal to f_y/E , and ϵ_{sh} and E_{sh} are the strain hardening strain and strain hardening modulus from the employed quad-linear



(a) Compression plus major axis bending



(b) Compression plus minor axis bending

Fig. 11. Calibration of the modified interaction factors $k_{yy,mod-EC3}$ and $k_{zz,mod-EC3}$ for S235 steel welded I-section beam-columns.

material model, as detailed in [36].

$$M_{y,csm} = \begin{cases} W_{pl,y} f_y \left[1 - \left(1 - \frac{W_{el,y}}{W_{pl,y}} \right) / \left(\frac{\epsilon_{csm}}{\epsilon_y} \right)^2 \right], & \text{for } \epsilon_{csm} \leq \epsilon_{sh} \\ W_{pl,y} f_y \left[1 - \left(1 - \frac{W_{el,y}}{W_{pl,y}} \right) / \left(\frac{\epsilon_{csm}}{\epsilon_y} \right)^2 + 0.08 \frac{E_{sh}}{E} \left(\frac{\epsilon_{csm} - \epsilon_{sh}}{\epsilon_y} \right)^2 \right], & \text{for } \epsilon_{csm} > \epsilon_{sh} \end{cases} \quad (25)$$

$$M_{z,csm} = \begin{cases} W_{pl,z} f_y \left[1 - \left(1 - \frac{W_{el,z}}{W_{pl,z}} \right) / \left(\frac{\epsilon_{csm}}{\epsilon_y} \right)^{1.2} \right], & \text{for } \epsilon_{csm} \leq \epsilon_{sh} \\ W_{pl,z} f_y \left[1 - \left(1 - \frac{W_{el,z}}{W_{pl,z}} \right) / \left(\frac{\epsilon_{csm}}{\epsilon_y} \right)^{1.2} + 0.05 \frac{E_{sh}}{E} \left(\frac{\epsilon_{csm} - \epsilon_{sh}}{\epsilon_y} \right)^2 \right], & \text{for } \epsilon_{csm} > \epsilon_{sh} \end{cases} \quad (26)$$

In Eqs. (25) and (26), ϵ_{csm} is the limiting CSM strain that defines the maximum strain that a cross-section can endure prior to failure, as determined from:

$$\frac{\epsilon_{csm}}{\epsilon_y} = \frac{0.25}{-3.6}, \text{ but } \frac{\epsilon_{csm}}{\epsilon_y} \leq \min \left(\Omega, \frac{0.4\epsilon_u}{\epsilon_y} \right) \text{ for } \bar{\lambda}_p \leq 0.68 \quad (27)$$

where Ω sets the maximum tolerable level of plastic strain, with a recommended value of 15, and $\bar{\lambda}_p$ is the cross-sectional slenderness defined by:

$$\bar{\lambda}_p = \sqrt{\frac{f_y}{\sigma_{cr,cs}}} \quad (28)$$

In Eq. (28), $\sigma_{cr,cs}$ is the elastic local buckling stress of the welded I-section in bending about the relevant axis, which can be obtained through numerical methods, such as the finite strip software CUFSM [44], or alternatively through the analytical formulae developed by Gardner et al. [38]. The CSM has been shown to yield more accurate and consistent bending moment capacity predictions for I-section profiles compared to the current EC3 and AISC design provisions [26,45]. The CSM is thus employed in the new beam-column design proposals to determine the bending end point of the interaction curves (i.e. Eqs. (25) and (26)). Based on the improved compression and bending end points, new interaction factors (i.e. $k_{yy,prop}$ and $k_{zz,prop}$ for the major and minor axis bending, respectively) are now calibrated using the numerical dataset derived in Section 2.3, as described in the following subsection.

4.2. Calibration of new interaction factors

Data for two cross-section sizes $100 \times 150 \times 10 \times 10$ and $100 \times 200 \times 12 \times 16$ ($B \times H \times t_f \times t_w$, in mm) with modified EC3 compressive load levels (i.e. $n_{mod-EC3,y}$ for major axis bending and $n_{mod-EC3,z}$ for minor axis bending, as defined by Eqs. (29) and (30), respectively) varying from 0.2 to 0.8, in increments of 0.2, were isolated from the full numerical database generated in Section 2.3 and used for the calibration of the new interaction factors $k_{yy,prop}$ and $k_{zz,prop}$.

$$n_{mod-EC3,y} = \frac{N_{Ed}}{N_{b,y,mod-EC3}} \quad (29)$$

$$n_{mod-EC3,z} = \frac{N_{Ed}}{N_{b,z,mod-EC3}} \quad (30)$$

The benchmark (target) FE interaction factors $k_{yy,FE}$ and $k_{zz,FE}$ for these considered beam-columns were back-calculated from the numerical results using Eqs. (31) and (32), respectively, which are rearranged forms of the newly proposed design formulae (i.e. Eqs. (18) and (19)).

$$k_{yy,FE} = (1 - n_{mod-EC3,y}) \frac{M_{csm}}{M_{Ed}} \quad (31)$$

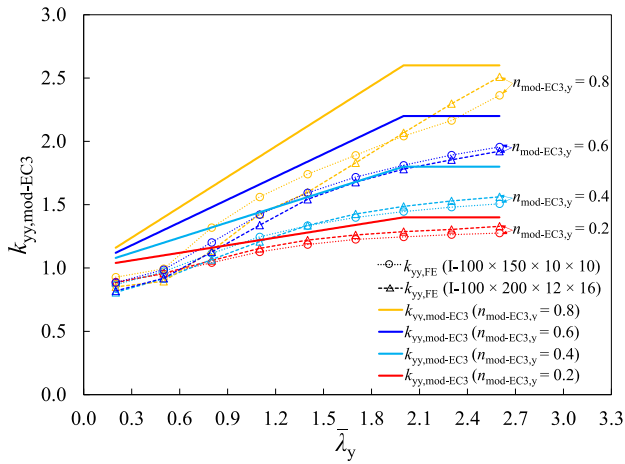
$$k_{zz,FE} = (1 - n_{mod-EC3,z}) \frac{M_{csm}}{M_{Ed}} \quad (32)$$

The numerically derived benchmark interaction factors $k_{yy,FE}$ and $k_{zz,FE}$ are plotted against the corresponding column non-dimensional slenderness $\bar{\lambda}$ for the four different compressive load levels $n_{mod-EC3}$ of 0.2, 0.4, 0.6 and 0.8 in Figs. 11–15 for beam-columns made of varying steel grades. Design formulae for the new interaction factors $k_{yy,prop}$ and $k_{zz,prop}$ are proposed based on these benchmark interaction factors $k_{yy,FE}$ and $k_{zz,FE}$, employing a bilinear form, in line with the current EC3 design approach [24,25], as expressed by Eqs. (33) and (34), respectively:

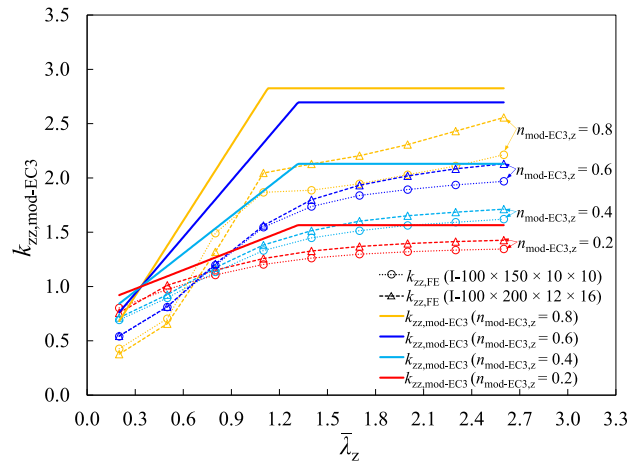
$$k_{yy,prop} = C_{my} \left[1 + D_{1,y} \left(\bar{\lambda}_y - D_{2,y} \right) n_{mod-EC3,y} \right] \leq C_{my} \left(1 + D_{3,y} n_{mod-EC3,y} \right) \quad (33)$$

$$k_{zz,prop} = C_{mz} \left[1 + D_{1,z} \left(\bar{\lambda}_z - D_{2,z} \right) n_{mod-EC3,z} \right] \leq C_{mz} \min \left(1 + D_{3,z} n_{mod-EC3,z}, D_{3,z} \right) \quad (34)$$

where $D_{1,y}$, $D_{1,z}$, $D_{2,y}$, $D_{2,z}$, $D_{3,y}$ and $D_{3,z}$ are coefficients that are determined through calibration against the numerically obtained datasets. The proposed coefficients are yield strength-dependent in order to capture the influence of yield strength on the shape of the interaction curves of welded I-sections made of varying steel grades, as summarised

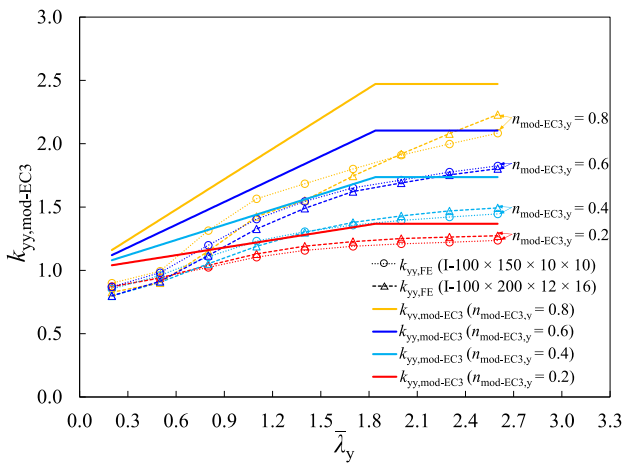


(a) Compression plus major axis bending

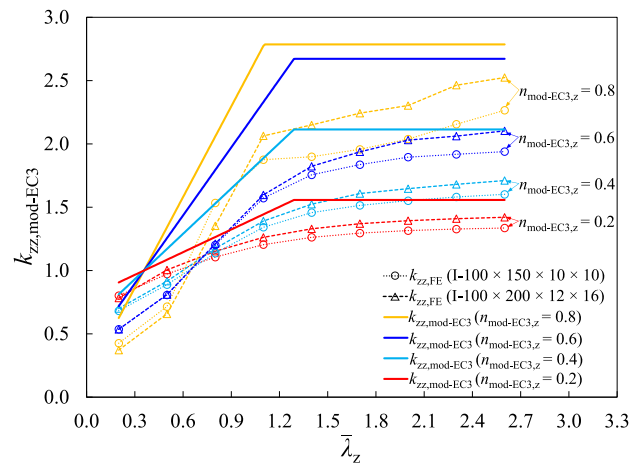


(b) Compression plus minor axis bending

Fig. 12. Calibration of the modified interaction factors $k_{yy,mod-EC3}$ and $k_{zz,mod-EC3}$ for S355 steel welded I-section beam-columns.

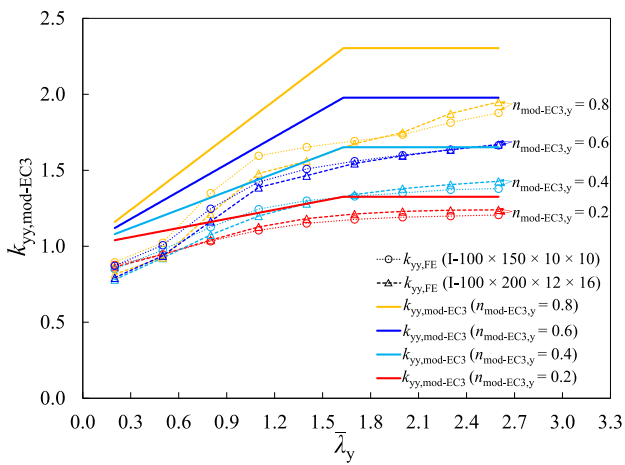


(a) Compression plus major axis bending

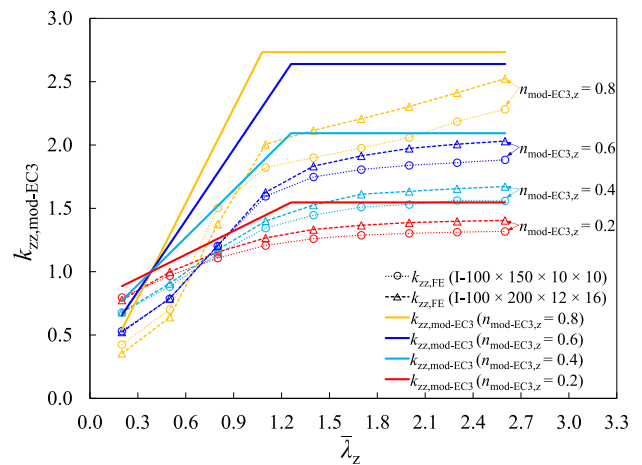


(b) Compression plus minor axis bending

Fig. 13. Calibration of the modified interaction factors $k_{yy,mod-EC3}$ and $k_{zz,mod-EC3}$ for S460 steel welded I-section beam-columns.

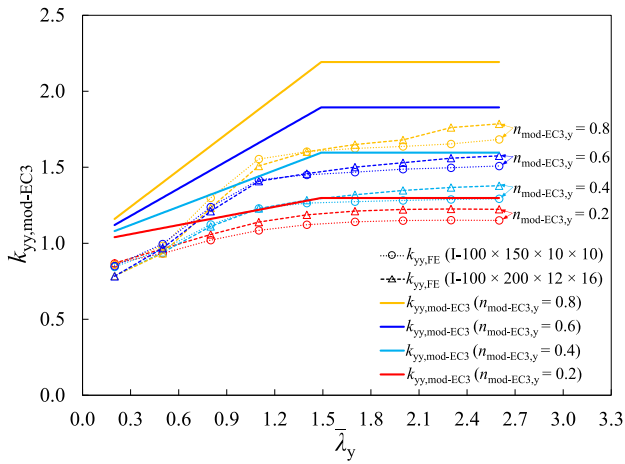


(a) Compression plus major axis bending

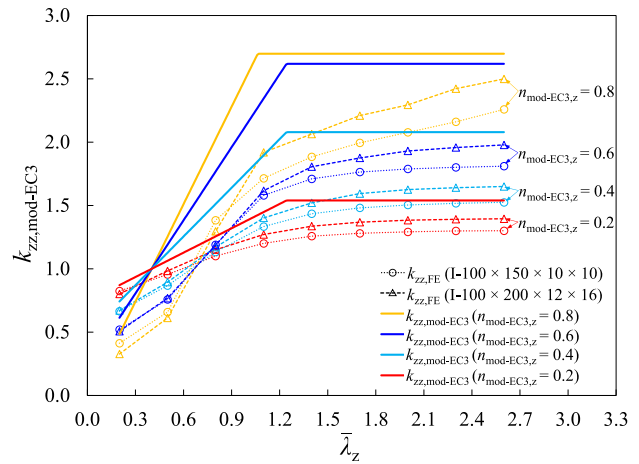


(b) Compression plus minor axis bending

Fig. 14. Calibration of the modified interaction factors $k_{yy,mod-EC3}$ and $k_{zz,mod-EC3}$ for S690 steel welded I-section beam-columns.



(a) Compression plus major axis bending



(b) Compression plus minor axis bending

Fig. 15. Calibration of the modified interaction factors $k_{yy,mod-EC3}$ and $k_{zz,mod-EC3}$ for S960 steel welded I-section beam-columns.

in Eq. (35) for $D_{1,y}$, $D_{2,y}$ and $D_{3,y}$ and Eq. (36) for $D_{1,z}$, $D_{2,z}$ and $D_{3,z}$.

$$\begin{cases} D_{1,y} = 1 \\ D_{2,y} = 0 \\ D_{3,y} = 1.6\epsilon + 0.7 \end{cases} \quad (35)$$

$$\begin{cases} D_{1,z} = 3.7 - \epsilon \\ D_{2,z} = 0.5 - 0.2\epsilon \\ D_{3,z} = 0.4\epsilon + 2.5 \end{cases} \quad (36)$$

The proposed interaction factors $k_{yy,prop}$ and $k_{zz,prop}$ are compared with the numerically derived benchmark interaction factors $k_{yy,FE}$ and $k_{zz,FE}$ in Figs. 11–15 for welded I-section beam-columns made of varying steel grades. It can be observed from Figs. 11–15 that the proposed interaction factors generally follow the trend of the benchmark FE data points and offer suitably safe-sided predictions, though there are relatively large discrepancies between the proposed and FE derived interaction factors for beam-columns with large slenderness values $\bar{\lambda}$ under high axial compressive load levels $n_{mod-EC3}$. However, these discrepancies have a very small influence on the accuracy of the resistance predictions since, at high axial load levels, the axial compression term (see Eqs. (18) and (19)) is dominant [23,46–48], while the bending term, which features the interaction factor, is small.

4.3. Assessment of new design proposals

The accuracy of the newly developed design proposals for NSS and HSS welded I-section beam-columns is evaluated through comparisons against the existing test data [20,21] and numerical results generated from the parametric studies described in Section 2.3. The ratios of $N_{u,FE(test)}/N_{u,pred,prop}$ are plotted against the corresponding angle parameter θ in Fig. 16(a) and (b) for beam-columns under compression plus major and minor axis bending, respectively. It can be observed from Fig. 16(a) and (b) that the new design proposals result in more accurate and less scattered ultimate resistance predictions for NSS and HSS non-slender welded I-section beam-columns than the current EC3 and AISC design provisions. As indicated in Tables 3 and 4, the mean ratios of $N_{u,FE(test)}/N_{u,pred,prop}$ are equal to 1.085 and 1.115 for beam-columns subjected to compression plus major and minor axis bending, respectively, with corresponding COV values equal to 0.035 and 0.048, which are significantly reduced compared to those of the current EC3 and AISC design provisions, highlighting the ability of the proposed method to provide more consistent resistance predictions for beam-columns made of steel grades varying from S235 to S960. Moreover, the new design proposals predict overall safe-sided ultimate resistance predictions for NSS and HSS welded I-section beam-columns, with only

Table 5

Variability parameters of material and geometric properties specified in prEN 1993-1-1 [24].

Parameter	X_m/X_n	V_x
f_y (S235)	1.25	0.055
f_y (S355)	1.20	0.050
f_y (S460)	1.15	0.045
f_y (above S460)	1.10	0.035
E	1.00	0.030
H	1.00	0.009
B	1.00	0.009
t_f	0.98	0.025
t_w	1.00	0.025

a very limited number of predictions on the unsafe side, as shown in Fig. 16. The significant improvements of the new design proposals over the existing EC3 and AISC design provisions are attributed to the adoption of the more accurate compression and bending end points, as well as the more accurate interaction curves calibrated against the numerically obtained results.

5. Reliability analysis

The reliability of the new design proposals for NSS and HSS non-slender welded I-section beam-columns is investigated through statistical analyses in line with EN 1990 [28] using the numerically obtained data from the parametric studies as well as the test data collected from the literature [20,21]. The key variability parameters of the basic material and geometric properties are taken from Annex E of prEN 1993-1-1 [24], as listed in Table 5, where X_m is the mean value of the variable, X_n is the nominal value of the variable and V_x is the corresponding COV of the variable. The COV of the cross-sectional area V_A can be determined on the basis of the variability parameters of the basic cross-sectional dimensions H , B , t_f and t_w following the method outlined in [49], which is, on average, equal to 0.02 for all the investigated welded I-sections.

The beam-column design formulae can be rewritten in the form of Eq. (37), where C_0 is a constant coefficient, and C_1 , C_2 and C_3 are the coefficients indicating the level of participation of the material yield strength f_y , cross-sectional area A and Young's modulus E , respectively, in the beam-column resistance predictions; these coefficients can be calculated following the method detailed in [49].

$$N_{b,R} = C_0 f_y^{C_1} A^{C_2} E^{C_3} \quad (37)$$

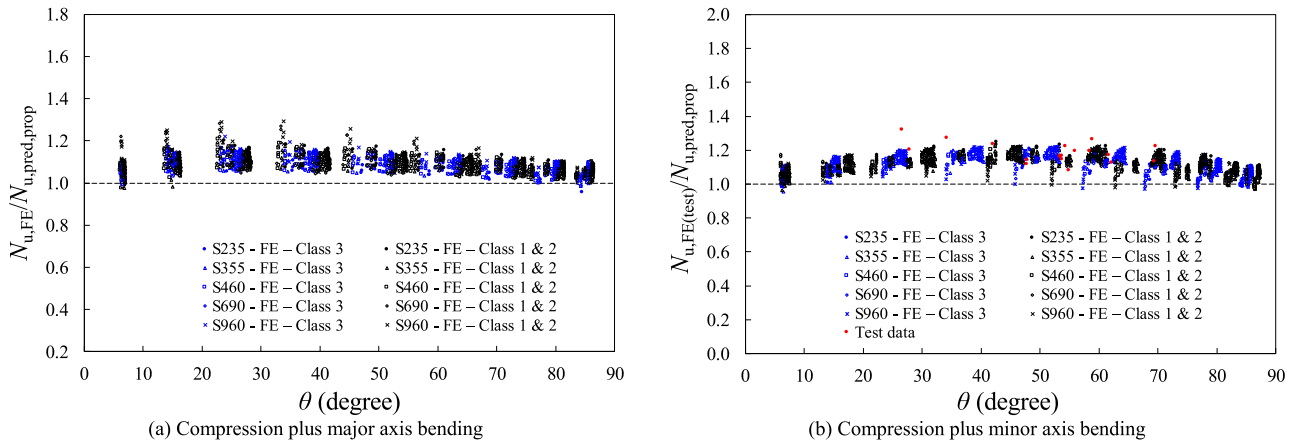


Fig. 16. Comparisons of FE and test results with resistance predictions determined using the new design proposals for NSS and HSS non-slender welded I-section beam-columns under combined loading.

Table 6

Key reliability analysis results for the new design proposals for NSS and HSS welded I-section beam-columns under compression plus major axis bending.

Steel grade	No. of FE data	<i>b</i>	<i>k_{d,n}</i>	<i>V_δ</i>	<i>γ_{M1}</i> *
S235	729	1.076	3.054	0.033	0.951
S355	729	1.077	3.054	0.032	0.970
S460	729	1.081	3.054	0.031	0.996
S690	729	1.090	3.054	0.035	1.018
S960	729	1.103	3.054	0.034	0.998
Overall	3645	1.085	3.042	0.034	1.014

Table 7

Key reliability analysis results for the new design proposals for NSS and HSS welded I-section beam-columns under compression plus minor axis bending.

Steel grade	No. of FE (test) data	<i>b</i>	<i>k_{d,n}</i>	<i>V_δ</i>	<i>γ_{M1}</i> *
S235	729	1.119	3.054	0.045	0.944
S355	729	1.108	3.054	0.047	0.967
S460	729 (14)	1.113	3.054	0.047	1.059
S690	729 (4)	1.113	3.054	0.049	1.031
S960	729	1.120	3.054	0.051	1.026
Overall	3645 (18)	1.115	3.042	0.048	1.026

The combined COV of the material and geometric basic variables *V_{rt}* can be then calculated using:

$$V_{rt} = \sqrt{(C_1 V_{f_y})^2 + (C_2 V_A)^2 + (C_3 V_E)^2} \tag{38}$$

Other key statistical parameters are also presented in Tables 6 and 7 for beam-columns made of varying steel grades under combined compression plus major axis bending and minor axis bending, respectively, where *n* is the number of the numerical and experimental data points used in the reliability analysis, *b* is the correction factor, *k_{d,n}* is the design fracture factor depending on the value of *n*, *V_δ* is the COV of the ratio of *N_{u,FE(test)}*/*N_{u,pred,prop}* and *γ_{M1}** is the required partial safety factor. Note that the correction factor *b* is determined using Eq. (39) instead of the least squares method recommended in EN 1990 [28] in order to prevent *b* being biased towards the numerical results of beam-columns with higher ultimate resistances [50,51], where *r_{e,i}* represents the numerical ultimate resistance and *r_{t,i}* represents the theoretical ultimate resistance determined using the new design proposals presented in Section 4.

$$b = \frac{1}{n} \sum_{i=1}^n \frac{r_{e,i}}{r_{t,i}} \tag{39}$$

It can be seen from Tables 6 and 7 that the required partial safety factors *γ_{M1}** for the newly proposed design method are lower than or

very close to the target value of 1.0 [24] for welded I-section beam-columns with varying steel grades. It can thus be concluded that the newly proposed design method can be safely applied to the design of NSS and HSS non-slender welded I-section beam-columns under compression plus uniaxial bending using the current EC3 partial safety factor of 1.0.

6. Conclusions

A comprehensive and systematic numerical modelling programme has been conducted in this paper to explore the behaviour and design of NSS and HSS non-slender welded I-section beam-columns subjected to compression plus uniaxial bending. FE models that can closely replicate the structural response of NSS and HSS welded I-section beam-columns were established and validated against existing test results from the literature [20,21]. The validated FE models were then utilised to conduct parametric studies considering a wide range of cross-section geometries, member slendernesses, steel grades and loading combinations. The numerically obtained results, as well as the test data collected from the literature [20,21], were employed to evaluate the accuracy of the current beam-column design methods provided in prEN 1993-1-1 [24], EN 1993-1-12 [1] and AISC 360-16 [2]. It was found that both the EC3 and AISC design methods yield somewhat scattered ultimate resistance predictions with inaccuracies arising in the endpoints of the interaction curves and the interaction curves themselves. To overcome the shortcomings in the existing design provisions, new beam-column design proposals were established, featuring the adoption of the recently proposed column buckling design method by Yun et al. [16] and the Continuous Strength Method (CSM) [26] for the calculation of the compression and bending end point resistances, respectively, together with newly devised interaction curves anchored to these more accurate end points. The new design proposals were shown to provide more accurate, consistent and generally safe-sided resistance predictions than the current design methods for non-slender welded I-section beam-columns made of steel grades varying from S235 to S960. The reliability of the new design proposals was also assessed by means of statistical analysis following the procedures provided in EN 1990 [28], confirming that the current EC3 partial safety factor of unity can be safely used.

CRedit authorship contribution statement

Yufei Zhu: Writing – original draft, Validation, Methodology, Investigation, Formal analysis. **Xiang Yun:** Writing – review & editing, Supervision, Methodology, Investigation, Formal analysis. **Leroy Gardner:** Writing – review & editing, Supervision, Funding acquisition.

Declaration of competing interest

The authors declare that they have no known competing financial interests or personal relationships that could have appeared to influence the work reported in this paper.

Data availability

Data will be made available on request.

Acknowledgement

This project has received funding from the Research Fund for Coal and Steel under grant agreement no. 743504.

References

- [1] EN 1993-1-12:2007, Eurocode 3: Design of Steel Structures – Part 1-12: Additional Rules for the Extension of EN 1993 Up to Steel Grades S700, European Committee for Standardization (CEN), Brussels, 2007.
- [2] ANSL/AISC 360-16, Specification for Structural Steel Buildings, American Institute of Steel Construction (AISC), Chicago, Illinois, 2016.
- [3] G. Shi, W.J. Zhou, Y. Bai, C.C. Lin, Local buckling of 460MPa high strength steel welded section stub columns under axial compression, *J. Constr. Steel Res.* 100 (2014) 60–70.
- [4] D.K. Kim, C.H. Lee, K.H. Han, J.H. Kim, S.E. Lee, H.B. Sim, Strength and residual stress evaluation of stub columns fabricated from 800MPa high-strength steel, *J. Constr. Steel Res.* 102 (2014) 111–120.
- [5] G. Shi, W. Zhou, C. Lin, Experimental investigation on the local buckling behavior of 960 MPa high strength steel welded section stub columns, *Adv. Struct. Eng.* 18 (2015) 423–437.
- [6] A. Su, Y. Sun, O. Zhao, Y. Liang, Local buckling of S960 ultra-high strength steel welded I-sections subjected to combined compression and major-axis bending, *Eng. Struct.* 248 (2021) 113213.
- [7] A. Su, Y. Sun, Y. Liang, O. Zhao, Experimental and numerical studies of S960 ultra-high strength steel welded I-sections under combined compression and minor-axis bending, *Eng. Struct.* 243 (2021) 112675.
- [8] Y. Sun, Y. Liang, O. Zhao, B. Young, Experimental and numerical investigations of S690 high-strength steel welded I-sections under combined compression and bending, *J. Struct. Eng.* 147 (2021) 04021054.
- [9] D. Beg, L. Hladnik, Slenderness limit of class 3 I cross-sections made of high strength steel, *J. Constr. Steel Res.* 38 (3) (1996) 201–217.
- [10] H. Bartsch, F. Eyben, G. Pauli, S. Schaffrath, M. Feldmann, Experimental and numerical investigations on the rotation capacity of high-strength steel beams, *J. Struct. Eng.* 147 (6) (2021) 04021067.
- [11] N. Schillo, M. Feldmann, Experiments on the rotational capacity of beams made of high-strength steel, *Steel Constr.* 11 (2018) 42–48.
- [12] Y.F. Zhu, X. Yun, L. Gardner, Behaviour and design of high strength steel homogeneous and hybrid welded I-section beams, *Eng. Struct.* 275 (2023) 115275.
- [13] H.Y. Ban, G. Shi, Y.Q. Shi, Y.J. Wang, Overall buckling behavior of 460MPa high strength steel columns: Experimental investigation and design method, *J. Constr. Steel Res.* 74 (2012) 140–150.
- [14] Y. Deng, S. Zhou, J. Li, S. Nie, P. Liu, Buckling behaviour of Q460GJ welded H-section columns subjected to minor axis under axial compression, *Structures* 34 (2021) 1416–1428.
- [15] T.J. Li, G.Q. Li, S.L. Chan, Y.B. Wang, Behavior of Q690 high-strength steel columns: Part 1: Experimental investigation, *J. Constr. Steel Res.* 123 (2016) 18–30.
- [16] X. Yun, Y.F. Zhu, X. Meng, L. Gardner, Welded steel I-section columns: Residual stresses, testing, simulation and design, *Eng. Struct.* 282 (2023) 115631.
- [17] K.J.R. Rasmussen, G.J. Hancock, Tests of high strength steel columns, *J. Constr. Steel Res.* 34 (1995) 27–52.
- [18] A. Su, Y. Liang, O. Zhao, Experimental and numerical studies of S960 ultra-high strength steel welded I-section columns, *Thin-Walled Struct.* 159 (2021) 107166.
- [19] A. Su, K. Jiang, M. Wang, O. Zhao, S960 ultra-high strength steel slender welded I-section beam-columns: Testing, numerical modelling and design, *Thin-Walled Struct.* 177 (2022) 109452.
- [20] B. Yang, L. Shen, S.B. Kang, M. Elchalakani, S.D. Nie, Load bearing capacity of welded Q460GJ steel H-columns under eccentric compression, *J. Constr. Steel Res.* 143 (2018) 320–330.
- [21] T.Y. Ma, Y.F. Hu, X. Liu, G.Q. Li, K.F. Chung, Experimental investigation into high strength Q690 steel welded H-sections under combined compression and bending, *J. Constr. Steel Res.* 138 (2017) 449–462.
- [22] T.Y. Ma, G.Q. Li, K.F. Chung, Numerical investigation into high strength Q690 steel columns of welded H-sections under combined compression and bending, *J. Constr. Steel Res.* 144 (2018) 119–134.
- [23] K. Tse, J. Wang, X. Yun, Structural behaviour and continuous strength method design of high strength steel non-slender welded I-section beam-columns, *Thin-Walled Struct.* 169 (2021) 108273.
- [24] prEN 1993-1-1:2019, Eurocode 3: Design of Steel Structures – Part 1-1: General Rules and Rules for Buildings, European Committee for Standardization (CEN), Brussels, 2019, Final document.
- [25] EN 1993-1-1:2005, Eurocode 3: Design of Steel Structures – Part 1-1: General Rules and Rules for Buildings, European Committee for Standardization (CEN), Brussels, 2005.
- [26] X. Yun, L. Gardner, N. Boissonnade, The continuous strength method for the design of hot-rolled steel cross-sections, *Eng. Struct.* 157 (2018) 179–191.
- [27] X. Yun, L. Gardner, The continuous strength method for the design of cold-formed steel non-slender tubular cross-sections, *Eng. Struct.* 175 (2018) 549–564.
- [28] EN 1990, Eurocode: Basis of Structural Design, European Committee for Standardization (CEN), Brussels, 2002.
- [29] Abaqus 2018, SIMULIA - Dassault Systèmes, 2018.
- [30] X. Yun, L. Gardner, N. Boissonnade, Ultimate capacity of I-sections under combined loading – Part 2: Parametric studies and CSM design, *J. Constr. Steel Res.* 148 (2018) 265–274.
- [31] J. Liu, S. Chen, T.M. Chan, Experimental and numerical investigations of hybrid high strength steel welded T-section stub columns with Q690 flange and Q460 web, *Thin-Walled Struct.* 177 (2022) 109403.
- [32] J. Liu, S. Chen, T.M. Chan, Testing, numerical modelling and design of Q690 high strength steel welded T-section stub columns, *Eng. Struct.* 259 (2022) 114142.
- [33] A. Fieber, L. Gardner, L. Macorini, Formulae for determining elastic local buckling half-wavelengths of structural steel cross-sections, *J. Constr. Steel Res.* 159 (2019) 493–506.
- [34] EN 1993-1-5:2006, Eurocode 3: Design of Steel Structures – Part 1-5: Plated Structural Elements, European Committee for Standardization (CEN), Brussels, 2006.
- [35] C. Quan, M. Kucukler, L. Gardner, Design of web-tapered steel I-section members by second-order inelastic analysis with strain limits, *Eng. Struct.* 224 (2020) 111242.
- [36] X. Yun, L. Gardner, Stress-strain curves for hot-rolled steels, *J. Constr. Steel Res.* 133 (2017) 36–46.
- [37] A. Su, Y. Sun, Y. Liang, O. Zhao, Membrane residual stresses and local buckling of S960 ultra-high strength steel welded I-section stub columns, *Thin-Walled Struct.* 161 (2021) 107497.
- [38] L. Gardner, A. Fieber, L. Macorini, Formulae for calculating elastic local buckling stresses of full structural cross-sections, *Structures* 17 (2019) 2–20.
- [39] T. Tankova, L. Simões da Silva, F. Rodrigues, Buckling curve selection for HSS welded I-section members, *Thin-Walled Struct.* 177 (2022) 109430.
- [40] X. Yun, X. Meng, L. Gardner, Design of cold-formed steel SHS and RHS beam-columns considering the influence of steel grade, *Thin-Walled Struct.* 171 (2022) 108600.
- [41] L. Gardner, X. Yun, F. Walport, The continuous strength method – Review and outlook, *Eng. Struct.* 275 (2023) 114924.
- [42] L. Gardner, F. Wang, A. Liew, Influence of strain hardening on the behavior and design of steel structures, *Int. J. Struct. Stab. Dyn.* 11 (5) (2011) 855–875.
- [43] L. Gardner, The continuous strength method, *Proc. Inst. Civ. Eng. - Struct. Build.* 161 (3) (2008) 127–133.
- [44] B. Schafer, S. Ádány, Buckling analysis of cold-formed steel members using CUFSM: conventional and constrained finite strip methods, in: *Proceedings of the 18th International Specialty Conference on Cold-Formed Steel Structures*, Orlando, FL, USA, 2006, pp. 39–54.
- [45] X. Lan, J. Chen, T.-M. Chan, B. Young, The continuous strength method for the design of high strength steel tubular sections in bending, *J. Constr. Steel Res.* 160 (2019) 499–509.
- [46] M. Kucukler, L. Gardner, In-plane structural response and design of duplex and ferritic stainless steel welded I-section beam-columns, *Eng. Struct.* 247 (2021) 113136.
- [47] X. Meng, L. Gardner, Testing, modelling and design of normal and high strength steel tubular beam-columns, *J. Constr. Steel Res.* 183 (2021) 106735.
- [48] Y. Bu, L. Gardner, Laser-welded stainless steel I-section beam-columns: Testing, simulation and design, *Eng. Struct.* 179 (2019) 23–36.
- [49] S. Afshan, P. Francis, N.R. Baddoo, L. Gardner, Reliability analysis of structural stainless steel design provisions, *J. Constr. Steel Res.* 114 (2015) 293–304.
- [50] F. Walport, L. Gardner, D.A. Nethercot, Equivalent bow imperfections for use in design by second order inelastic analysis, *Structures* 26 (2020) 670–685.
- [51] X. Meng, L. Gardner, A.J. Sadowski, J.M. Rotter, Elasto-plastic behaviour and design of semi-compact circular hollow sections, *Thin-Walled Struct.* 148 (2020) 106486.